

WATER ADSORPTION IN HYDROPHILIC ZEOLITES: EXPERIMENT AND SIMULATION

*Juan Manuel Castillo¹, Joaquín Silvestre Albero², Francisco Rodríguez-Reinoso²,
Thijs J.H. Vlugt³, and Sofia Calero⁴*

¹*Laboratory of Engineering Thermodynamics, Erwin-Schrödinger-straße 44,
University of Kaiserslautern, 67663Kaiserslautern, Germany*

²*Laboratorio de Materiales Avanzados, Departamento de Química Inorgánica, Universidad de Alicante,
Ctra. San Vicente-Alicante s/n, Ap. 99, E- 03080 Alicante, Spain*

³*Department of Process and Energy, Delft University of Technology,
Leeghwaterstraat 44, 2628CA Delft, The Netherlands*

⁴*Faculty of Experimental Sciences, University Pablo de Olavide, Ctra. de Utrera km. 1, 41013 Sevilla, Spain*

We have measured experimental adsorption isotherms of water in zeolite LTA4A, and studied the regeneration process by performing subsequent adsorption cycles after degassing at different temperatures. We observed incomplete desorption at low temperatures, and cation rearrangement at successive adsorption cycles. We also developed a new molecular simulation force field able to reproduce experimental adsorption isotherms in the range of temperatures between 273 K and 374 K. Small deviations observed at high pressures are attributed to the change of the water dipole moment at high loadings. The force field correctly describes the preferential adsorption siting of water at different pressures. We tested the influence of the zeolite structure, framework flexibility, and cation mobility when considering adsorption and diffusion of water. Finally, we performed checks on force field transferability between different hydrophilic zeolite types, concluding that classical, non-polarizable water force fields are not transferable.

Introduction

The adsorption of water in hydrophilic zeolites is an important process in the purification of wastewater, catalysis, and gas separation. In particular, zeolite LTA4A is widely used to separate polar from non-polar molecules by permeation, as this zeolite is highly hydrophilic due to its low Si/Al ratio¹. For example, LTA4A has proven to be useful in alcohol dehydration²⁻⁴, pollutant removal from water^{5,6}, or even as working medium in the refrigeration of thermal machines⁷.

Experimental adsorption isotherms of water in zeolites provided by different research groups often show large deviations^{8,9}, mainly due to imperfections in the zeolite crystals, cation relocation, or indetermination in the location of the Al atoms in the zeolite structure¹⁰. Therefore, it is important to compare different experimental sets to make sure that the adsorption data reported is consistent and reproducible. Molecular simulation studies also reveal large differences in adsorption depending on the simulation parameters and the models employed. In a previous work¹¹, we studied water adsorption in hydrophobic zeolites by molecular simulation. We showed that water adsorption was extremely sensitive to small changes in the force field parameters, the selection of water model, the position of the framework atoms, and the partial charges of the zeolite atoms. There is a large number of simulation studies on the adsorption of water in different hydrophilic zeolites, mostly in FAU^{12,13} and MFI^{14,15}, but also in others such as HEU¹⁶, GOO¹⁷, or MOR¹⁸. Many of them focus on the description of the cation and water adsorption sites, which are not very sensitive to the force field parameters. It is still unknown whether it is possible to develop a classical, general force field able to correctly describe the adsorption of water in any hydrophilic zeolite. Although some research groups have used a determined force field to study adsorption in different hydrophilic zeolites^{19,20}, it is not clear if these force fields can reproduce the adsorption isotherms for different zeolites at different conditions. It has been shown that the adsorption calculated by molecular simulation in zeolites with non framework cations depends on the specific location of the alumina atoms in the structure²¹, which is usually unknown. In the case of the LTA4A zeolite, which has a Si/Al ratio equal to one, the location of the non-framework cations is well known. In this zeolite, the positions of the silicon and alumina atoms alternate following the Lowenstein's rule, which forbids the bonding of two alumina atoms by an oxygen atom.

Another reason to focus on this particular zeolite is that it has been extensively studied both experimentally^{1,9}, and by molecular simulation. Furukawa *et al.*²² used a rigid model of LTA4A with fixed cations and blocked beta cages to study adsorption and diffusion of water, ethanol, and their mixtures. These authors found large water adsorption selectivity, and a larger diffusion of

water compared to ethanol, which is unable to cross the 8-ring windows of the structure. Jaramillo *et al.*²³ studied the adsorption and adsorption siting as a function of loading of water and other small molecules in LTA4A, using a rigid model where the non-framework cations did not move from their crystallographic positions. Although not explicitly compared with experimental data, their water adsorption is too large, probably due to the large partial charges of the framework atoms. Kristof *et al.*²⁴ simulated the adsorption of water, methanol, and their mixtures in LTA4A, showing the importance of water hydrogen bonding for adsorption. They found that adsorption takes place in two steps: a first layer close to the zeolite wall, and then a second layer on top of the first. In their simulations water molecules cannot enter the beta cages, because this is only allowed by translation moves and the diffusion through the 6-ring windows is very slow. Wu *et al.*²⁵ studied the adsorption and diffusion of water/alcohol mixtures in LTA4A with a fully flexible zeolite model. They report adsorption with deviations of up to 10% respect to the experimental data, while the molecules are not able to enter the beta cages. Faux *et al.*²⁶ perform Molecular Dynamics (MD) simulations to describe molecular siting. These authors conclude that there are four water molecules adsorbed in every beta cage, that the diffusion through the 6-rings is very slow, and that the water structure is very similar to the bulk water structure at short distances. Gren *et al.*²⁷ also use MD simulations with a polarizable model for water, zeolite, and cations, to study the adsorption on the external surface of LTA4A. They observe adsorption by layers, and the leaching of the cations out of the zeolite. A similar approach was used by Allen *et al.*²⁸ to study the adsorption and diffusion of water on the external surface of LTA4A, which was modeled with terminal silanol groups. Higgings *et al.*²⁹ used energy minimization methods to study molecular siting, concluding that the beta cage is the most stable site for water adsorption.

The structure of zeolite LTA4A is shown in Figure 1. It consist of sodalite, or beta cages, joined to each other in a cubic arrangement by 4 membered rings. The sodalite cages are accessible via 6 membered rings windows, only large enough to allow the diffusion of cations, water, and other few small atoms/molecules. The void space between sodalite cages is called alpha cage. Alpha cages are connected by 8 membered ring windows. The extra framework sodium cations of the zeolite are initially located in the dehydrated structure at three different adsorption sites: site I, at the center of the 6-rings; site II, on the plane of the 8-rings; site III, facing the 4-rings³⁰.

Here we study water adsorption in the hydrophilic zeolite LTA4A, which has the advantage that the location of the framework atoms in the zeolite is unique and exactly known. We measure experimental adsorption isotherms, and create a new force field for guest-host interactions that can reproduce the experimental adsorption by molecular simulation. We test the influence of cation

mobility in two different framework characterizations of LTA4A^{30,31}, demonstrating the importance of cation rearrangement during adsorption. We check the ability of the new force field for describing water adsorption in different hydrophilic zeolites, and conclude that more refined models are needed to obtain a general force field for water adsorption in hydrophilic zeolites. Finally, we provide possible explanations to the deviation of our simulation results respect to the experiment at high pressures.

Methods

A commercial NaA zeolite supplied by Linde (zeolite Type A with LTA structure) has been used in this work. Zeolite A has a typical unit cell composition of $(\text{Na}_{12}[\text{Al}_{12}\text{Si}_{12}\text{O}_{48}] \cdot 27 \text{H}_2\text{O})_8$, with a Si/Al ratio close to 1.0. The NaA zeolite crystals have an average size of 44 nm, as deduced from XDR analysis. Water adsorption isotherms were performed in house made volumetric equipment (LMA-hydrosorb) equipped with one pressure transducer (1000 torr). Water adsorption isotherms were measured at 298 K and 334 K and up to $p/p_0 \sim 1.0$ (water vapor pressure = 23.8 torr and 156.5 torr, respectively). Before each adsorption measurement, zeolite samples were degassed at 573 K overnight under UHV conditions. Consecutive adsorption cycles were performed in order to analyze the regeneration of the zeolite NaA. A degassing treatment was performed in between cycles using different temperatures (423 K, 523 K and 573 K) for 4h.

Adsorption isotherms were calculated by molecular simulations in the grand-canonical ensemble, where the temperature, volume and chemical potential of the system are constant³². The chemical potential is directly related to the fugacity, which can be computed from the pressure and a given equation of state. Here we will consider the ideal gas approximation for water, as the pressures considered were lower than 10 kPa. The insertion/deletion of molecules was performed using the Configurational-Bias Monte Carlo technique³³, and the following Monte Carlo moves used for the water molecules: insertion/deletion of molecules (1/3 of the moves); regrow, translation, rotation, and random translation (1/6 of the moves for each type of move). Cation movement was achieved by translation and random translation movements (both movements with the same probability). The maximum translation and rotation distances were adjusted during the simulation to achieve an average acceptance probability of 50%. Simulations were performed in cycles, every cycle containing a number of Monte Carlo moves equal to the number of molecules present in the system, with a minimum of 20^{34,35}. We performed additional Molecular Dynamics simulations with mobile cations in the canonical ensemble to determine if there is diffusion through the windows accessing

the beta cages³⁶. The equations of movement were integrated using the Verlet algorithm with a time step of 0.5 fs during a minimum of 20 million production cycles. The temperature of the system was controlled with a Nosé-Hoover chain thermostat of length 3. The energy drift in the simulations was negligible.

We used the rigid Tip5pEw³⁷ water model and an existent force field for the description of the zeolite³⁸. In a previous work¹¹, we justified the use of this water model for studying the adsorption of water in zeolites. The water-zeolite and water-cation interactions were fitted to the experimental data obtained in this work. Two different characterizations of the LTA4A structure, hydrated and dehydrated, were used in the study to describe the atomic positions of the zeolite^{30,31}. We used the characterizations of Fitch *et al.*³⁹ and Olson⁴⁰ to assign positions to the atoms of the FAU zeolite, and selected a random distribution of alumina atoms satisfying the Lowenstein's rule. The simulation box consisted of a single unit cell of zeolite. The cell was kept rigid in most calculations. In the simulations with flexible framework the bonded interactions were described by the Nicholas model⁴¹. The model of Garcia-Sanchez *et al.*³⁸ was used to assign point charges to the zeolite atoms. The extra framework cations that balance the net charge of the zeolite were initially placed at the crystallographic positions of their respective structure^{30,31}, and either allowed to move, or left fixed. The Lennard-Jones interactions were truncated and shifted at a cut-off radius of 12Å. Electrostatic interactions were calculated using the Ewald summation technique with a precision of 10⁻⁶⁴². The non-bonded parameters of the force field used in this work are summarized in Table 1.

Results and Discussion

Figure 2 shows the experimental adsorption isotherms at 334 K for a different number of adsorption cycles (Figure 2 a-c), and degassing temperatures of 423 K, 523 K, and 573 K (Figure 2 d-f). The adsorption is clearly different between different cycles at the same degassing temperature, and at the same cycle and different degassing temperature. The adsorption is always lower in the first cycle, while in successive cycles the adsorption is basically the same (see Figure 2a-c). Larger differences occur at lower pressures, and in the case of the lowest degassing temperature (Figure 2a) there are clear deviations also at high pressures. This last effect is attributed to incomplete degassing, as it has been estimated that complete water desorption can only be achieved at temperatures larger than 423 K¹, and some authors even suggest temperatures in the vicinity of 700 K⁴³. Incomplete desorption **can** affect the isotherms at low pressures, as preadsorbed water **molecules act as** extra adsorption sites, increasing the adsorption capacity of the zeolite **in** the

subsequent measurements. However, water adsorption will not be enhanced if these hydrated cations are not accessible, as it occurs in the first adsorption cycle. A different situation occurs when the pristine zeolite has been already exposed to water at saturation pressure, i.e. after the first cycle. Water adsorption can give rise to reallocation of the extra framework cations of the zeolite to more favorable positions, making them more accessible to water molecules and therefore increasing the adsorption capacity in subsequent cycles. It is well known that cations act as nucleation centers for water molecules, and that they reallocate in the presence of water^{44,45}. In the rest of the study we will compare adsorption isotherms obtained by molecular simulation with the experimental adsorption isotherms obtained after several regeneration cycles, using a degassing temperature of 573 K.

To test the validity of our experiments, we compare our adsorption isotherms to other experimental adsorption data taken from the literature at 298 K and 334 K (Figure 3 and 4 respectively). Our adsorption isotherms match the experimental isotherms of Gorbach *et al.*⁹ and Morris⁴⁶ at both temperatures. Small deviations can be attributed to the fact that these isotherms were measured for the pelletized form of the zeolite, while we measured them in zeolite crystals. Although the effect of the binder is considered to be negligible due to its low surface area⁴⁶, its effect in the adsorption is difficult to evaluate and it should not be completely ignored. The rest of the experimental data presented in Figs. 3 and 4^{8,47,48} deviates from the matching isotherms, and we will neglect them in the present study.

We fit the guest-host interactions of the force field to reproduce the experimental water adsorption isotherm in LTA4A at different temperatures, using mobile cations and the hydrated structure. The fitting procedure was a mixture of trial and error and the use of the downhill simplex algorithm⁴⁹. The result is presented in Figure 5. Although our force field reproduces the general shape of the isotherm and the location of the condensation step in a large range of temperatures, it does not reproduce simultaneously the adsorption at low and high pressures. The interactions of water in a zeolite are different at high and low pressures. At low pressure, the water-zeolite interactions are dominant, while at high pressure the water-water interactions are more important⁵⁰. This is also reflected in the fact that the structure of water at saturation conditions is very similar to the structure of bulk water²⁶. The differences between simulation and experiment at high pressures can be attributed to the increase of the water dipole moment inside the zeolite when the loading increases. The importance of polarizability in the arrangement of adsorbed molecules in zeolites has been previously suggested⁵¹. Coudert *et al.*¹⁹ demonstrated by Carr-Parrinello molecular dynamics simulations that the dipole moment of water molecules adsorbed in hydrophilic zeolites increases

with loading, up to values similar to the dipole moment of bulk water. The Tip5pEw water model used in this study has a fixed dipole moment of 2.29 D^{37} , and therefore it does not take into account this effect. As the water dipole moment increases the adsorption increases, because the water-zeolite/water-cation interactions become stronger. This result was checked by some test simulations that artificially increased the dipole moment of water only at high pressure conditions by increasing the atomic partial charges of the water model. The calculated isotherm at 334 K perfectly matches the experimental isotherm at low pressures, while at higher pressures the adsorption is lower. At 1 kPa, the deviation between the simulation and the experiment is of around 20%. This large deviation disappears if we increase the water dipole to a value of 2.5 D (Fig. 6). It is difficult to provide a more precise value due to the large error bars in the adsorption at high loadings. This larger value of the dipole moment is consistent with the dipole moment calculated for water at similar loadings in hydrophilic LTA-type zeolites, estimated in 2.9 D^{19} . Nevertheless, we do not have any guarantee that this artificial water model with an increased dipole moment would lead to an accurate description of bulk water properties. Calculation of adsorption in hydrophilic zeolites using polarizable water models will be the topic of a future study.

We investigated the influence of cation mobility and zeolite structure by calculating adsorption isotherms at 334 K at different simulation conditions, see Figure 6. When the cations are mobile, there is no difference in adsorption between the hydrated and the dehydrated structure. The pore volume of the two structures calculated by molecular simulation is very similar ($4005 \text{ \AA}^3/\text{unit cell}$ for the hydrated structure, $4000 \text{ \AA}^3/\text{unit cell}$ for the dehydrated structure), and we do not expect a large difference in saturation adsorption between the two structures. The maximum difference between the atomic positions of the hydrated and dehydrated structure is 0.194 \AA . These differences are enough to have an effect in the adsorption of water in hydrophobic structures¹¹, but not in hydrophilic zeolites. In hydrophilic zeolites, water adsorbs preferentially coordinated to the extra framework cations, so that the influence of the detailed framework position is not so important.

The adsorption with fixed cations is lower than with mobile cations in both structures. This suggests that the mobile cations rearrange during the simulation to locations different from their initial positions, which is an often observed phenomenon in this and other zeolites^{3,52}. The influence of cation mobility is large for the whole pressure range, which clearly shows the importance of considering cation mobility in the simulations. The adsorption with fixed and mobile cations is similar only in the dehydrated structure at low pressures. These results indicate that mobile cations at these conditions do not move far from their crystallographic positions. For example, at 1 Pa the maximum average displacement of a cation from its crystallographic position is 2 \AA . Initially, there

are four cations inside every beta cage in the dehydrated structure, and three in the hydrated structure. During the hydration process, one of the cations inside the beta cage in the dehydrated structure migrates out of the cage. Therefore, more water molecules can be adsorbed in these cages, which are their preferential adsorption site as it was demonstrated both experimentally^{1,43} and by simulation²⁹. This migration takes place when there are between 25 and 30 water molecules adsorbed per unit cell of LTA4A (1.8 – 2.2 mol/kg).

Adsorption in the beta cages of LTA4A is limited by diffusion through 6-ring windows. Monte Carlo simulations do not have this limitation, as with this simulation method the molecules can easily overcome large free energy barriers. To establish if the force field here developed allows water to be adsorbed in the beta cages, which experimentally is the preferential adsorption site, it is necessary to perform a diffusion study by Molecular Dynamics. In this study, a LTA4A zeolite is filled with water molecules located in the alpha cage and equilibrated, checking at all times that during this process no molecules move to the beta cages. Afterwards, we run a MD simulation of at least 10 ns, and count the number of molecules that diffuse to the beta cages. In the rigid structure no water molecule diffuses to the beta cage during the whole simulation time, while in the flexible zeolite the beta cages can easily accommodate three water molecules after only 15 ps, which enter the beta cages and leave them several times during the simulation. The explanation is that the 6-ring windows are too narrow even for the small water molecules to diffuse, and they can only cross the windows if they are allowed to breathe.

The question now is whether framework flexibility has any influence in water adsorption. It has been demonstrated that the influence of framework flexibility on the computed adsorption of small alkane molecules in zeolites is negligible⁵³, but this has not been clearly established for water. In Fig. 6 we show the comparison between the adsorption isotherm in both rigid and flexible LTA4A, for both the hydrated and dehydrated structure with mobile cations. The flexible zeolite model only provides a slightly larger adsorption than the rigid, often within the error bars of the simulation. We can conclude that water behaves like other small molecules, and that zeolite flexibility is important for diffusion because water can only cross narrow windows when the zeolite is flexible, but it does not have much influence in adsorption.

The water adsorption siting is also consistent with experimental data, as shown in the density surface plots of Figure 7. At low pressures, water molecules first occupy the beta cages. This is due to the fact that these cages offer water a better confined environment. A few molecules also adsorb

at the walls of the alpha cage. At higher pressures, water fills also the alpha cages, first the walls and then the center of the cage.

Finally, we test the transferability of force fields for describing water adsorption in hydrophilic zeolites. In Figure 8, we show computed water adsorption isotherms in LTA4A at 298 K using the force field described by Fuchs *et al.*⁵⁴, which perfectly reproduces water adsorption in a FAU type zeolite for different temperatures. Simulations were performed with both the Tip5pEw water model³⁷, and the Tip4p water model⁵⁵ originally used by Fuchs *et al.*⁵⁴. The adsorption provided by this force field is much larger than the experimental isotherm, and the isotherm calculated with the force field developed in this work. The main reason is that the force field of Fuchs was developed to reproduce water adsorption only in the FAU zeolite. Notice also that the partial charges of the framework atoms Fuchs' model are more than twice higher than in our model. Therefore, the water-zeolite interaction is more intense and the adsorption higher. We also calculated the adsorption in a FAU-type zeolite containing 52 sodium cations per unit cell at 300 K, and compared it with reference data⁵⁵ in Figure 9. We used the characterizations of Fitch *et al.*³⁹ and Olson⁴⁰ to assign positions to the atoms of the zeolite, and selected a random distribution of alumina atoms satisfying the Lowenstein's rule. The adsorption isotherms in both structures overlap. The original force field does not perform as well as in the reference⁵⁴, as the calculated adsorption in FAU-type zeolites depends on the specific location of alumina atoms in the zeolite²¹, which is not provided in the reference data. The force field developed in this work provides a lower water adsorption in hydrophylic zeolites than the force field of Fuchs *et al.*, resulting in a worse description of water adsorption in the FAU zeolite, but an excellent agreement with the LTA4A water isotherms.

Conclusions

The experimental water adsorption isotherms in LTA4A at different regeneration cycles show that the adsorption is always lower in the first cycle compare to successive cycles, and the same cycle and lower temperatures. This provides a clear evidence of a complete desorption at low temperatures, and a possible cation reallocation upon water adsorption. We developed a new force field for water adsorption in LTA4 that successfully reproduces experimental isotherms. The low adsorption at high pressures is attributed to the increase of the water dipole moment at conditions similar to bulk liquid water, which cannot be reproduced with our non-polarizable model. Contrarily to what happens in hydrophobic zeolites, water adsorption is not largely influenced by small changes in the zeolite structure, as in hydrophilic zeolites cations act as adsorption centers.

Therefore, cation mobility has a large effect in adsorption: when the cations are kept fixed at their crystallographic positions, they cannot migrate to more favorable positions upon the adsorption of water, and the water adsorption is lower than when the cations are mobile. We have shown that the preferential adsorption sites in the zeolite are the beta cages, in complete agreement with experimental data. We found that water molecules can only diffuse to the beta cages when the framework model is flexible, while adsorption is not influenced by framework flexibility. Finally, we concluded that force fields developed to reproduce water adsorption in hydrophilic zeolites are in general not transferable between different zeolite types. Therefore, when studying water adsorption in hydrophilic zeolites it is necessary to develop specific force fields for specific zeolite types taking into account the particular location of alumina atoms in the structure, or more refined force fields that can account for properties such as molecular polarization.

Table 1. Non-bonded force field parameters used in this work. O_{Al} represent oxygen atoms of the zeolite bonded to at least one Al atom; O_{Si} represent oxygen atoms of the zeolite bonded only to Si atoms; O_w , water oxygen atoms; M is the dummy atom in the Tip5pEw water model³⁷. The LTA4A zeolite only contains oxygen atoms of type O_{Al} .

Atom/s	$\epsilon/k_B / K$	$\sigma / \text{Å}$	q / e
Si	-	-	0.786
Al	-	-	0.486
O_{Al}	-	-	-0.414
O_{Si}	-	-	-0.393
Na	251.780	3.1440	0.383
O_w	89.516	3.0970	-
H	-	-	0.241
M	-	-	-0.241
$O_{Al} - Na$	33.000	3.2000	
$O_{Al} - O_w$	13.710	3.3765	
$O_{Si} - Na$	33.000	3.2000	
$O_{Si} - O_w$	13.710	3.3765	
$Na - O_w$	75.000	2.3900	

Figure 1. Structure of the dehydrated LTA4A zeolite³⁰. Yellow, silicon atoms; green, alumina atoms; red, oxygen atoms. The initial cation adsorption sites are marked with circles. This figure will appear in color in the electronic version of this article.

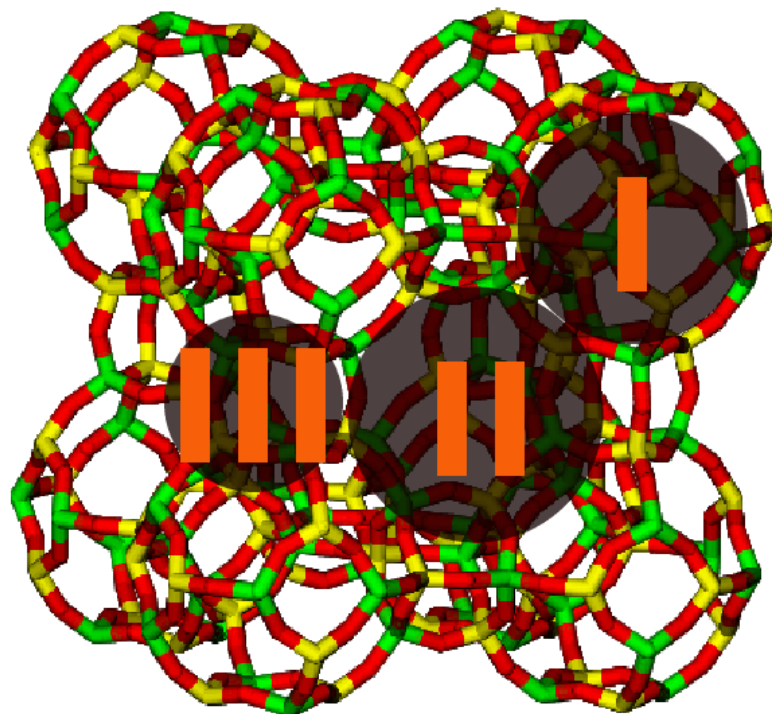


Figure 2. Experimental adsorption isotherms of water in LTA4A at 334 K. Left column: comparative of different cycles after degassing at (a) 423 K, (b) 523 K and (c) 723 K; Closed symbols, first adsorption cycle; open symbols, second adsorption cycle; crossed symbols, third adsorption cycle; Right column: comparative of the degassing temperature for the (d) first, (e) second and (f) third cycle; squares, degassing temperature of 423 K; triangles, degassing temperature of 523 K; diamonds, degassing temperature of 573 K.

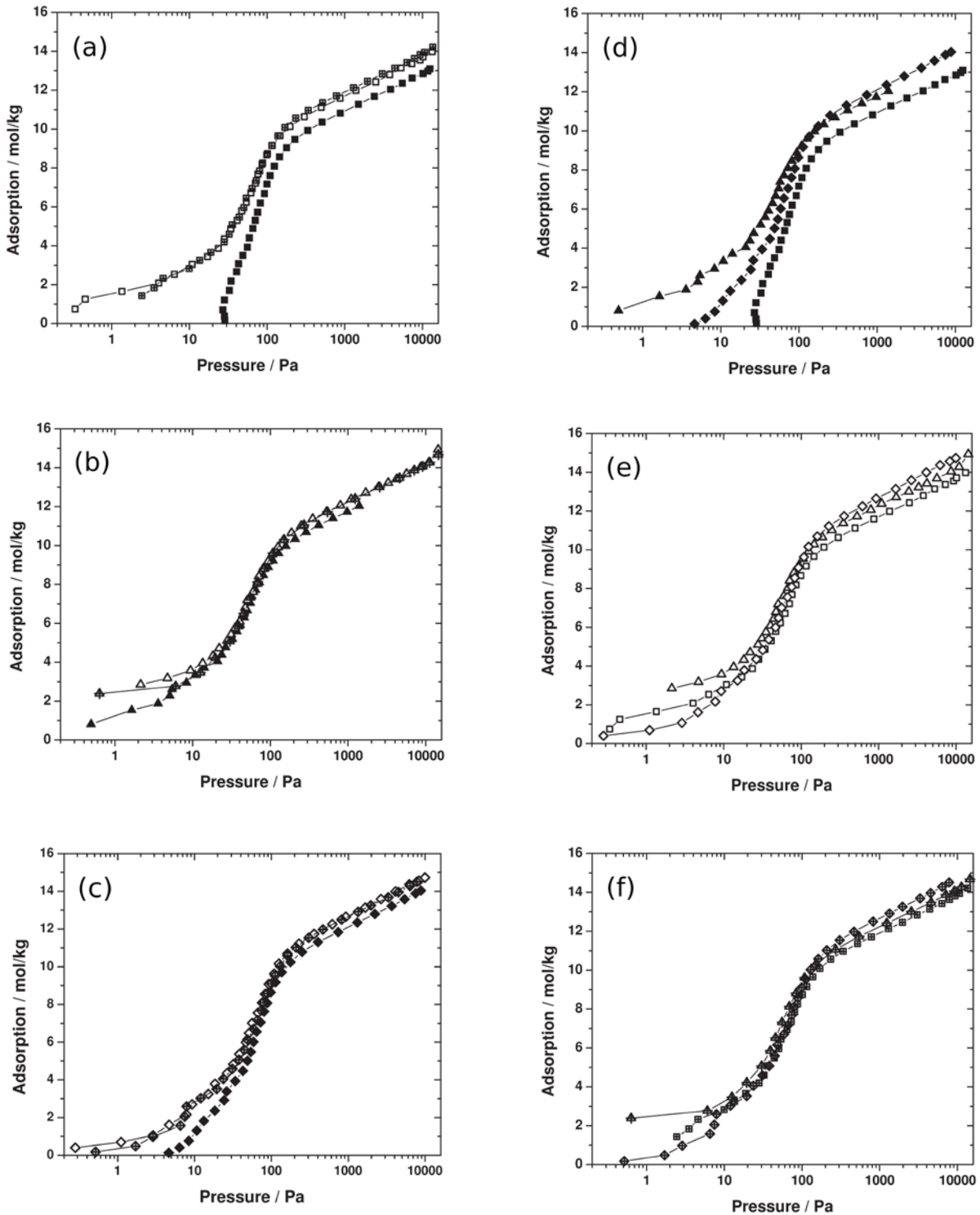


Figure 3. Experimental adsorption isotherms of water in LTA4A at temperatures close to 298 K. Squares, this work (298 K); circles, data of Gorbach *et al.*⁹ (298 K); triangles, data of Morris⁴⁶ (298 K); triangles down, data of Okamoto *et al.*⁸ (298 K); diamonds, data of Valiullin *et al.*⁴⁷ (300 K).

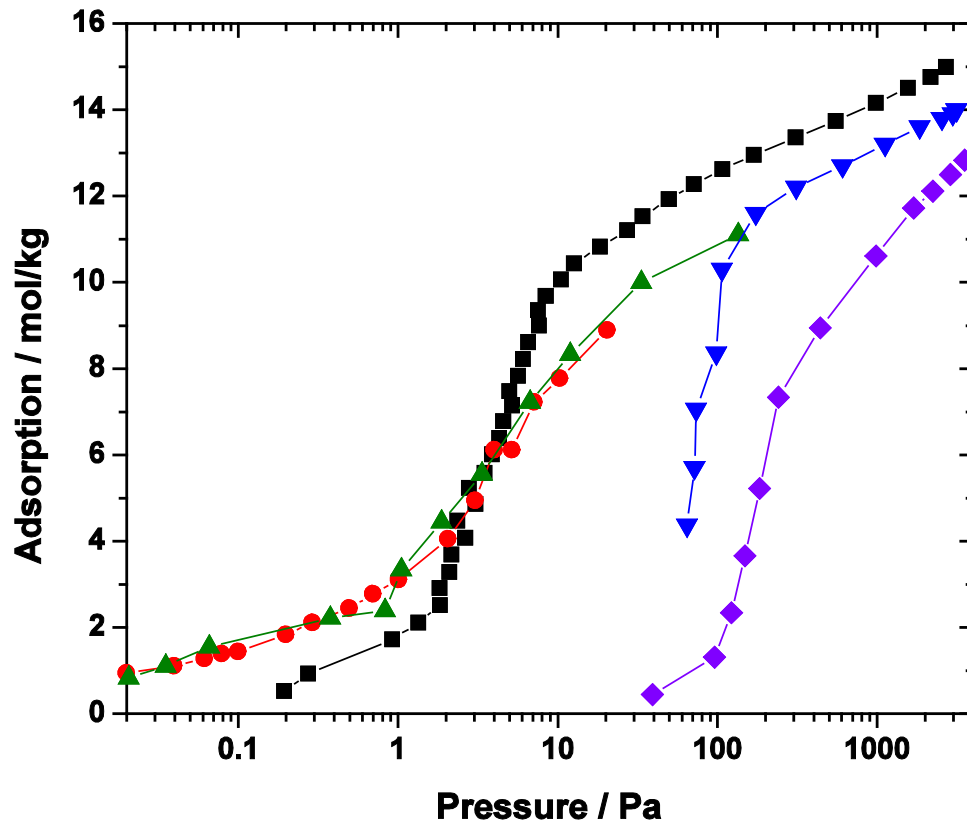


Figure 4. Experimental adsorption isotherms of water in LTA4A at temperatures close to 334 K. Squares, this work (334 K); circles, data of Gorbach *et al.*⁹ (334 K); triangles, data of Morris⁴⁶ (338 K); triangles down, data of Pera-Titus *et al.*⁴⁸ (333 K).

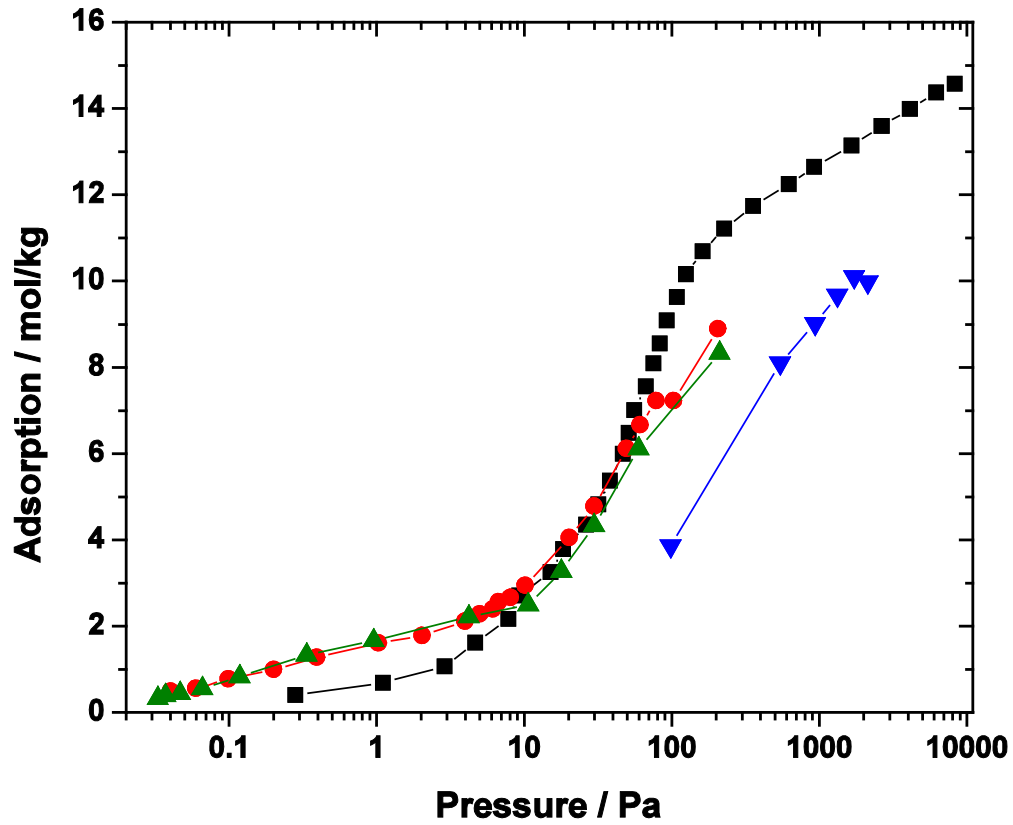


Figure 5. Adsorption isotherms of water in LTA4A calculated with the fitted force field parameters (open symbols) in the hydrated structure, and compared with experimental data (closed symbols), at different temperatures: squares, 273 K (experimental data from Gorbach *et al.*⁹); circles, 298 K; triangles, 334 K; diamonds, 374 K (experimental data from Grobach *et al.*⁹). Error bars are within the symbol size.

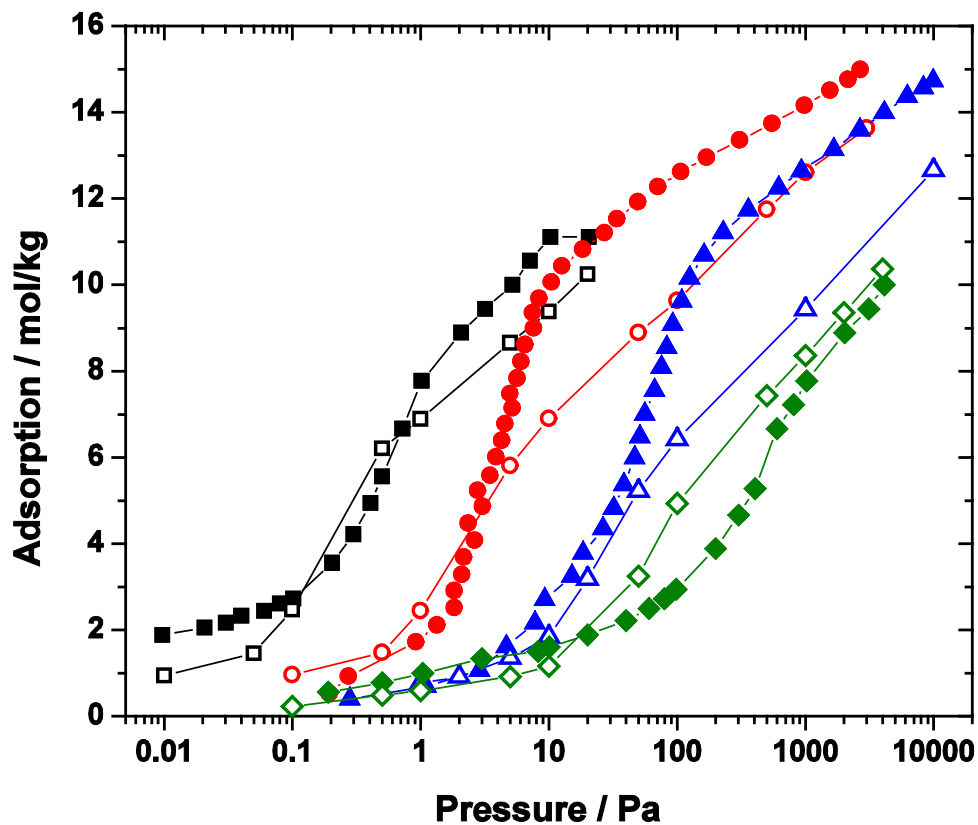


Figure 6. Adsorption isotherms of water in LTA4A at 334 K, calculated with different simulation parameters. Squares, experimental data; circles, hydrated structure; triangles, dehydrated structure; closed symbols, mobile cations; open symbols, fixed cations; crossed symbols, flexible structure with mobile cations; asterisk, hydrated structure with mobile cations, and a water dipole moment of 2.5 D. Error bars are within the symbol size.

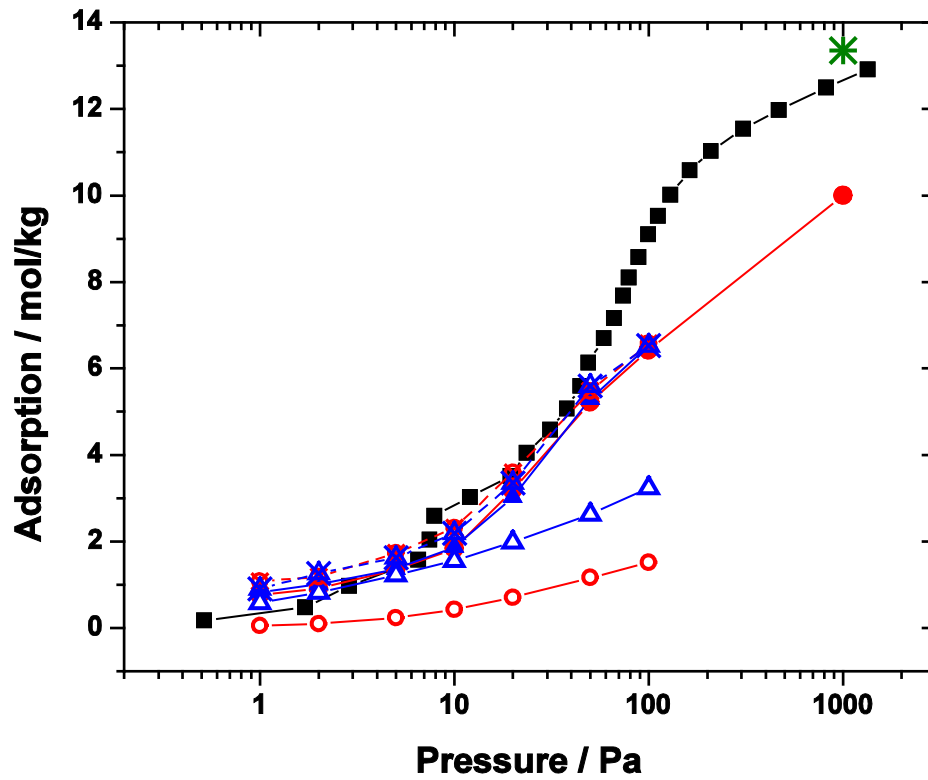


Figure 7. Water density plots in the hydrated LTA4A structure at 334 K and different pressures of water in the vapor phase. Top, 1Pa; bottom, 100Pa.

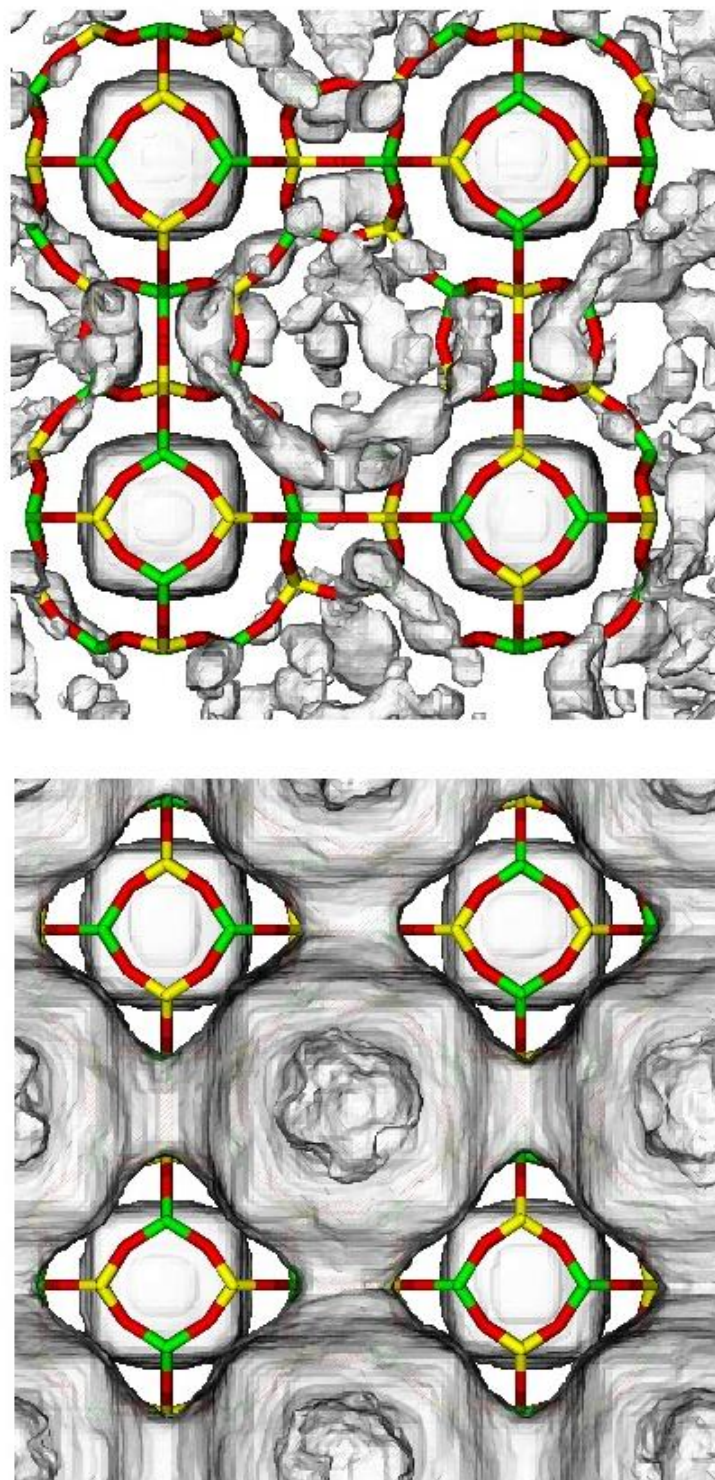


Figure 8. Adsorption isotherms of water in the hydrated structure of LTA4A at 298 K. Squares, experimental data; triangles, simulations using the force field developed in this work; diamonds, simulations using the force field by Fuchs *et al*⁵⁴ and the Tip5pEw³⁷ water model; triangles down, simulations using the force field by Fuchs *et al*⁵⁴ and the Tip4p water model⁵⁵. Cations are mobile in the simulations. Error bars are within the symbol size.

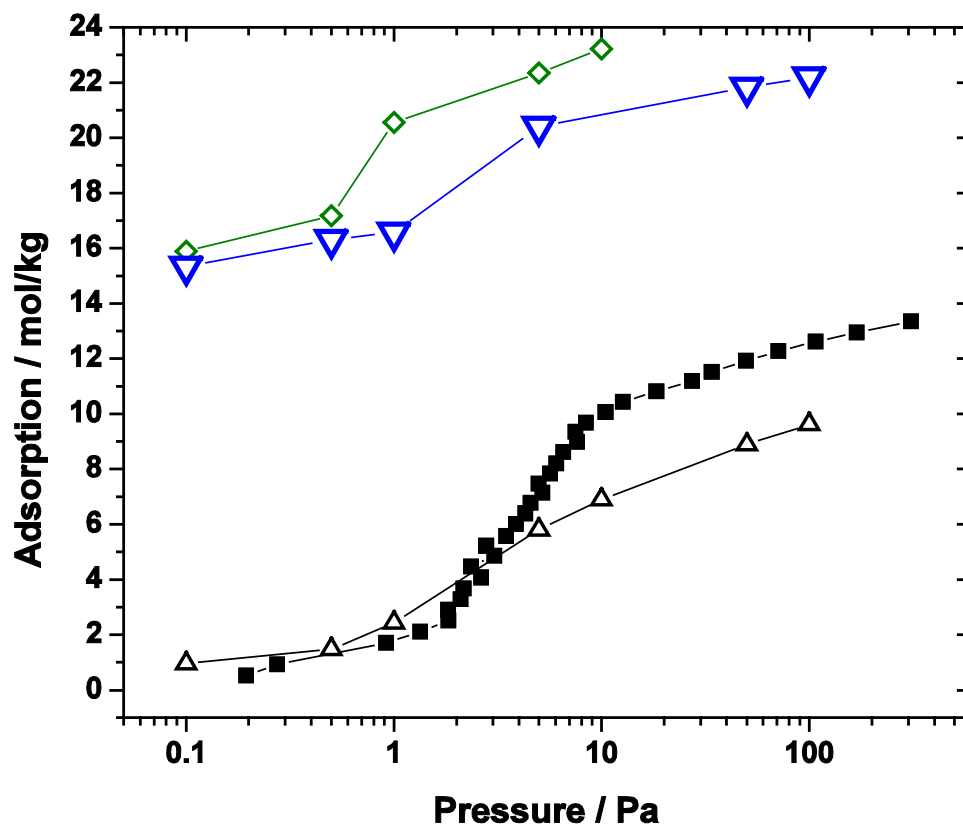
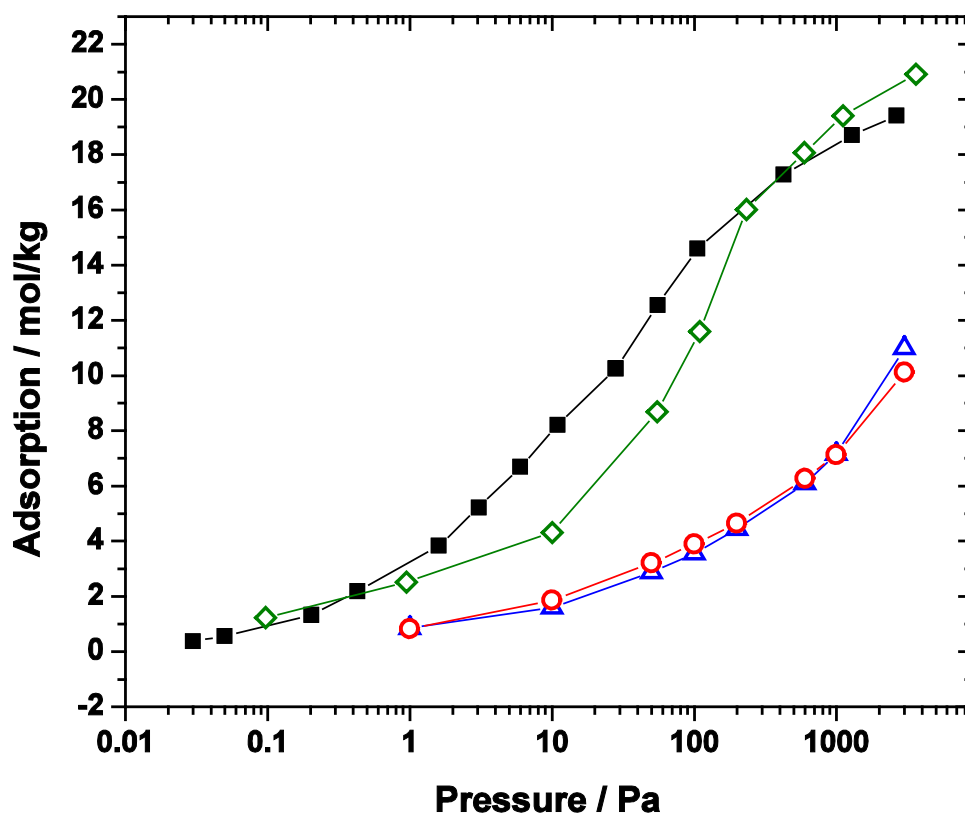


Figure 9. Adsorption isotherms of water in FAU containing 52 sodium cations per unit cell at 300 K, calculated using different simulation parameters. Squares, experimental data⁵⁵; triangles, simulations using the force field developed in this work and the Fick structure³⁹; circles, simulations using the force field developed in this work and the Olson structure⁴⁰; diamonds, simulations using the force field by Fuchs *et al*⁵⁴ (the water model used is Tip4p⁵⁵). Error bars are within the symbol size.



Acknowledgements

The authors would like to acknowledge A. Silvestre-Albero and E. Gadea for their help with the water adsorption measurements, the European Research Council through an ERC Staring Grant (Sofia Calero), and the MICINN (CTQ2010-16077) project.

References

- (1) Zhu, W.; Gora, L.; van den Berg, A. W. C.; Kapteijn, F.; Jansen, J. C.; Moulijn, J. A. *Journal of Membrane Science* **2005**, *253*, 57.
- (2) Huang, A.; Yang, W.; Liu, J. *Separation and Purification Technology* **2007**, *56*, 158.
- (3) Kyotani, T.; Ikeda, T.; Saito, J.; Nakane, T.; Hanaoka, T.; Mizukami, F. *Industrial & Engineering Chemistry Research* **2009**, *48*, 10870.
- (4) Li, Y. S.; Chen, H. L.; Liu, J.; Li, H. B.; Yang, W. S. *Separation and Purification Technology* **2007**, *57*, 140.
- (5) Liang, H.; Gao, H.; Kong, Q.; Chen, Z. *Journal of Chemical and Engineering Data* **2007**, *52*, 695.
- (6) Camargo Fernandes-Machado, N. R.; Malachini Miotto-Bigatao, D. M. *Quimica Nova* **2007**, *30*, 1108.
- (7) Adell, A.; Petrissans, J. *Talanta* **1998**, *45*, 777.
- (8) Okamoto, K.; Kita, H.; Horii, K.; Tanaka, K.; Kondo, M. *Industrial & Engineering Chemistry Research* **2001**, *40*, 163.
- (9) Gorbach, A.; Stegmaier, M.; Eigenberger, G. *Adsorption-Journal of the International Adsorption Society* **2004**, *10*, 29.
- (10) Liu, B.; Garcia-Perez, E.; Dubbeldam, D.; Smit, B.; Calero, S. *Journal of Physical Chemistry C* **2007**, *111*, 10419.
- (11) Castillo, J. M.; Dubbeldam, D.; Vlugt, T. J. H.; Smit, B.; Calero, S. *Molecular Simulation* **2009**, *35*, 1067.
- (12) Bellat, J. P.; Paulin, C.; Jeffroy, M.; Boutin, A.; Paillaud, J. L.; Patarin, J.; Di Lella, A.; Fuchs, A. *Journal of Physical Chemistry C* **2009**, *113*, 8287.
- (13) Abrioux, C.; Coasne, B.; Maurin, G.; Henn, F.; Boutin, A.; Di Lella, A.; Nieto-Draghi, C.; Fuchs, A. H. *Adsorption-Journal of the International Adsorption Society* **2008**, *14*, 743.
- (14) Guo, X. D.; Huang, S. P.; Teng, J. W.; Xie, Z. K. *Acta Physico-Chimica Sinica* **2006**, *22*, 270.
- (15) Yazaydin, A. O.; Thompson, R. W. *Microporous and Mesoporous Materials* **2009**, *123*, 169.
- (16) Channon, Y. M.; Catlow, C. R. A.; Gorman, A. M.; Jackson, R. A. *Journal of Physical Chemistry B* **1998**, *102*, 4045.
- (17) Ruiz-Salvador, A. R.; Almora-Barrios, N.; Gomez, A.; Lewis, D. W. *Physical Chemistry Chemical Physics* **2007**, *9*, 521.
- (18) Maurin, G.; Bell, R. G.; Devautour, S.; Henn, F.; Giuntini, J. C. *Journal of Physical Chemistry B* **2004**, *108*, 3739.
- (19) Coudert, F.-X.; Cailliez, F.; Vuilleumier, R.; Fuchs, A. H.; Boutin, A. *Faraday Discussions* **2009**, *141*, 377.
- (20) Di Lella, A.; Desbiens, N.; Boutin, A.; Demachy, I.; Ungerer, P.; Bellat, J. P.; Fuchs, A. H. *Physical Chemistry Chemical Physics* **2006**, *8*, 5396.
- (21) Garcia-Perez, E.; Dubbeldam, D.; Liu, B.; Smit, B.; Calero, S. *Angewandte Chemie-International Edition* **2007**, *46*, 276.

- (22) Furukawa, S.; Goda, K.; Zhang, Y.; Nitta, T. *Journal of Chemical Engineering of Japan* **2004**, *37*, 67.
- (23) Jaramillo, E.; Chandross, M. *Journal of Physical Chemistry B* **2004**, *108*, 20155.
- (24) Kristof, T.; Csanyi, E.; Rutkai, G.; Merenyi, L. *Molecular Simulation* **2006**, *32*, 869.
- (25) Wu, J. Y.; Liu, Q. L.; Xiong, Y.; Zhu, A. M.; Chen, Y. *Journal of Physical Chemistry B* **2009**, *113*, 4267.
- (26) Faux, D. A.; Smith, W.; Forester, T. R. *Journal of Physical Chemistry B* **1997**, *101*, 1762.
- (27) Gren, W.; Parker, S. C.; Slater, B.; Lewis, D. W. *Journal of Physical Chemistry C*, *114*, 9739.
- (28) Allen, J. P.; Gren, W.; Molinari, M.; Arrouvel, C.; Maglia, F.; Parker, S. C. *Molecular Simulation* **2009**, *35*, 584.
- (29) Higgins, F. M.; de Leeuw, N. H.; Parker, S. C. *Journal of Materials Chemistry* **2002**, *12*, 124.
- (30) Pluth, J. J.; Smith, J. V. *Journal of the American Chemical Society* **1980**, *102*, 4704.
- (31) Gramlich, V.; Meier, W. M. *Zeitschrift Fur Kristallographie Kristallgeometrie Kristallphysik Kristallchemie* **1971**, *133*, 134.
- (32) Pathria, R. K. *Statistical Mechanics*, Second ed.; Butterworth-Heinemann: Oxford, 1996; Vol. 1.
- (33) Siepmann, J. I.; Frenkel, D. *Molecular Physics* **1992**, *75*, 59.
- (34) Calero, S.; Dubbeldam, D.; Krishna, R.; Smit, B.; Vlugt, T. J. H.; Denayer, J. F. M.; Martens, J. A.; Maesen, T. L. M. *Journal of the American Chemical Society* **2004**, *126*, 11377.
- (35) Vlugt, T. J. H.; Krishna, R.; Smit, B. *Journal of Physical Chemistry B* **1999**, *103*, 1102.
- (36) Frenkel, D.; Smit, B. *Understanding Molecular Simulations: From Algorithms to Applications*, 2nd ed.; Academic Press: San Diego, 2002.
- (37) Rick, S. *Journal of Chemical Physics* **2004**, *120*, 6085.
- (38) Garcia-Sanchez, A.; Ania, C. O.; Parra, J. B.; Dubbeldam, D.; Vlugt, T. J. H.; Krishna, R.; Calero, S. *Journal of Physical Chemistry C* **2009**, *113*, 8814.
- (39) Fitch, A. N.; Jobic, H.; Renouprez, A. *Journal of Physical Chemistry* **1986**, *90*, 1311.
- (40) Olson, D. H. *Zeolites* **1995**, *15*, 439.
- (41) Nicholas, J. B.; Hopfinger, A. J.; Trouw, F. R.; Iton, L. E. *Journal of the American Chemical Society* **1991**, *113*, 4792.
- (42) Allen, M. P.; Tildesley, D. J. *Computer Simulations of Liquids*; Clarendon Press: Oxford, 1987.
- (43) Vucelic, V.; Vucelic, D.; Karaulic, D.; Susic, M. *Thermochimica Acta* **1973**, *7*, 77.
- (44) Goryainov, S. V.; Secco, R. A.; Huang, Y.; Liu, H. *Physica B-Condensed Matter* **2007**, *390*, 356.
- (45) Ohgushi, T.; Ishimaru, K.; Adachi, Y. *Journal of Physical Chemistry C* **2009**, *113*, 2468.
- (46) Morris, B. *Journal of Colloid and Interface Science* **1968**, *28*, 149.
- (47) Valiullin, R.; Kaerger, J.; Cho, K.; Choi, M.; Ryoo, R. *Microporous and Mesoporous Materials* **2011**, *142*, 236.
- (48) Pera-Titus, M.; Fite, C.; Sebastian, V.; Lorente, E.; Llorens, J.; Cunill, F. *Industrial & Engineering Chemistry Research* **2008**, *47*, 3213.
- (49) Nelder, J. A.; Mead, R. *Computer Journal* **1965**, *7*, 308.
- (50) Simonot-Grange, M. H.; Belhamidi-El Hannouni, F. *Thermochimica Acta* **1984**, *77*, 311.
- (51) Halasz, I.; Kim, S.; Marcus, B. *Molecular Physics* **2002**, *100*, 3123.
- (52) Beauvais, C.; Boutin, A.; Fuchs, A. H. *Comptes Rendus Chimie* **2005**, *8*, 485.
- (53) Vlugt, T. J. H.; Schenk, M. *Journal of Physical Chemistry B* **2002**, *106*, 12757.

- (54) Fuchs, A. H.; Boutin, A.; Teuler, J. M.; Di Lella, A.; Wender, A.; Tavitian, B.; Ungerer, P. *Oil & Gas Science and Technology-Revue D Ifp Energies Nouvelles* **2006**, *61*, 571.
- (55) Jorgensen, W. L.; Chandrasekhar, J.; Madura, J. D.; Impey, R. W.; Klein, M. L. *Journal of Chemical Physics* **1983**, *79*, 926.